Check for updates

Accepted Article

Polymer-Assisted Compressed Flux Growth: A Universal and High-Yield Method for Dimension-Controlled Single Crystals

Chao Ge[1,2,†], *Xiaoxin Zheng*[1,†], *Qing Guo*[1], *Yang Liu*[1,*], *and Xutang Tao*[1,*]

[1]State Key Laboratory of Crystal Materials, Shandong University, Jinan, 250100, China

[2]Institute of Laser Engineering, Faculty of Materials and Manufacturing, Beijing University of Technology, Beijing, 100124, China

*Corresponding author. Email: liuyangicm@sdu.edu.cn; txt@sdu.edu.cn

[†]These authors contributed equally to this work.

Keywords: crystal growth, compressed flux growth, polymer flux, high-yield, dimensional controllability

Abstract:

Single crystals possess the most perfect and stable morphology, and represent the intrinsic and upper limits of performance when integrated into various application scenarios. However, for a large portion of the newly emerging low-dimensional and molecular materials, the mass production of crystals with a desirable shape is still challenging. Here, we provide a universal and high-yield method to grow functional single crystals with controlled dimensions that could be directly integrated into a device. By utilizing a polymeric flux in combination with a compressed growth space, numerous materials can be grown into size-controllable single crystalline flakes, with millions

This article has been accepted for publication and undergone full peer review but has not been through the copyediting, typesetting, pagination and proofreading process, which may lead to differences between this version and the Version of Record. Please cite this article as doi: 10.1002/adma.202210685.

This article is protected by copyright. All rights reserved.

15214095, ja, Downloaded from https://onlinelibrary.wiley.com/doi/10.1002/adma.202210685 by CochraneChina, Wiley Online Library on [06/01/2023]. See the Terms and Conditions (https://onlinelibrary.wiley.com/terms-and-conditions) on Wiley Online Library for rules of use; OA articles are governed by the applicable Creative Commons License

produced in one batch. This scalable growth method shows promise for the large-scale integration of micro-single crystals as functional components, as exemplified by the construction of a 5-inch field effect transistor array.

1. Introduction

The preparation of single crystals with specific morphologies is one of the cornerstones of many high-tech sectors,[1–4] ranging from casting an alloy into single-crystal turbine blades for jet engines to the photoetching of single-crystal silicon wafers to produce logic and memory chips.[5, 6] To meet the developing demands of further miniaturization and flexibility, the micro/nano-scale crystals of a series of emergent functional materials have become optimal platforms for the construction of active layers.[7–10] However, the well-developed crystal growth techniques such as the Czochralski method for silicon ingots and flux method utilizing a melt of a metal or inorganic compound as a solvent are difficult to use for low-dimensional and organic molecular materials.[11–13] At the same time, they are not sufficient to realize the large-scale production of micro/nano-crystals.[14, 15] Although researchers have developed a series of solution- and vapor-based techniques to control the assembly of molecules or precursors,[16–18] cost-effective crystallization methods capable of controlling the crystallinity and dimensional uniformity are still being pursued[19, 20].

This study developed a high-yield method to grow single crystals with controlled dimensions that could be directly integrated into devices. This method, which is coined compressed flux growth (CFG), combines a polymer flux (e.g., silicone oil) with a compressed growth space. CFG possesses various merits, including (i) overcoming the solubility limitations, and thus being applicable to a wide range of materials even with low solubility, weak stability, and poor crystallization capacity; (ii) producing quasi-two-dimensional flakes regardless of the intrinsic dimensions of the crystal habits, with a uniform lateral size and thickness tuned from tens to hundreds of nanometers; and (iii) high productivity with hundreds of thousands of single crystalline flakes per square centimeter. As a versatile and scalable method to realize the large-batch growth of uniform low-dimensional crystals, we regard CFG as a pivotal method for the mass production of functional crystal-based devices via a brand-new construction strategy.

This article is protected by copyright. All rights reserved.

Accepted Article

15214095, ja, Downloaded from https://onlinelibrary.wiley.com/doi/10.1002/adma.202210685 by CochraneChina, Wiley Online Library on [06/01/2023]. See the Terms and Conditions (https://onlinelibrary.wiley.com/terms-and-conditions) on Wiley Online Library for rules of use; OA articles are governed by the applicable Creative Commons License

Accepted Article

15214095, ja, Downloaded from https://onlinelibrary.wiley.com/doi/10.1002/adma.202210685 by CochraneChina, Wiley Online Library on [06/01/2023]. See the Terms and Conditions (https://onlinelibrary.wiley.com/terms-and-conditions) on Wiley Online Library for rules of use; OA articles are governed by the applicable Creative Commons License

2. Results and Discussion

2.1 Compressed Flux Growth of Pentacene Single Crystalline Flakes

The CFG apparatus is schematically depicted in **Figure 1a**. The growth is implemented on a home-made thermocompressor equipped with a bottom flat heater and an upper hydraulic piston to simultaneously provide an asymmetric vertical thermal field and static pressure. The growth system is sandwiched between two compressed substrates (silicon, glass, quartz, etc.). The adoption of a specific polymer as the flux is a crucial factor for the CFG to guarantee the crystal growth. Here, we take silicone oil (polydimethylsiloxane)[21, 22] as a most representative polymer flux to illustrate the CFG procedure by growth of single crystalline flakes of a superstar organic semiconductor, pentacene[23, 24]. The temperature program for the growth procedure and status of the mixture at each stage are shown in **Figure 1b**. Here, silicone oil (with a dynamic viscosity of 60,000 mPa.s) acts as a high-temperature flux. Only above a critical temperature (depending on the ratio of pentacene to silicone, but normally >200 °C), its polydimethylsiloxane chains have adequate intermolecular forces to break the cohesive energy of the pentacene solids to realize dissolution. The adoption of the polymer flux makes the almost impossible solution-crystallization of pentacene a highly effective process, with a nearly 100% recovery yield. The confinement of the growth media with a static pressure (normally 100–300 kPa) between the compressed substrates not only protects the sensitive pentacene from oxidation and degradation, but also controls the crystalline morphology to produce ultrathin flakes with a unified thickness. After the growth was complete, it was found that nearly all of the crystalline flakes were stuck to the upper substrate (**Figure S2**), because its relatively low temperature generated nucleation. The effects of the feeding recipe and growth conditions on the grown crystalline flakes are illustrated in the Section 1 of Supporting Information and will be discussed in the following sections.

To evaluate the growth efficiency, morphology, and quality of the crystals, characterizations of the as-grown pentacene crystalline flakes are shown in **Figures 1c–i**. CFG produces massive crystalline flakes in one batch, with the number-density and average lateral size dependent on the target material-to-silicone oil ratio and cooling rate. With a pressure of 200 kPa, concentration of 30 mg ml^{-1}, and cooling rate of 20 °Cmin^{-1}, flakes were produced at approximately 1.35×10^5 per square

This article is protected by copyright. All rights reserved.

centimeter, with the lateral size concentrated in the range of 40–70 μm (inset of **Figure 1c**). The optical microscopy (OM) and cross-polarized microscopy (PM) images of the rhomboid flakes shown in **Figures 1c** and **1d**, respectively, indicate that they were evenly distributed throughout the substrate. When we scrutinized a flake by rotating it relative to the axis of the polarizer, its color and luminous intensity changed continuously and periodically from blue through magenta to red, while remaining homogeneous across the entirety, demonstrating the superb single-crystalline nature of each flake (**Figure 1e**). Scanning electron microscopy (SEM) and atomic force microscopy (AFM) images (**Figures 1f** and **1g**, respectively) show the sharp edges and smooth surface of the pentacene crystalline flakes grown under above-mentioned conditions, which had a root mean square roughness (Rq) of ~0.237 nm and thickness of ~70 nm. The selected area electron diffraction (SAED) pattern (**Figure 1h**) in the transmission electron microscopy (TEM) characterization exhibited bright and well-defined electron diffraction spots, reflecting the high crystallinity of the pentacene flakes. The indexing of these diffraction spots conformed to the triclinic P-*1* space group of pentacene, which was further verified using X-ray diffraction (XRD) (**Figure 1i**), with (001) as the main crystal plane.

This article is protected by copyright. All rights reserved.

Accepted Article

15214095, ja, Downloaded from https://onlinelibrary.wiley.com/doi/10.1002/adma.202210685 by CochraneChina, Wiley Online Library on [06/01/2023]. See the Terms and Conditions (https://onlinelibrary.wiley.com/terms-and-conditions) on Wiley Online Library for rules of use; OA articles are governed by the applicable Creative Commons License

Accepted Article

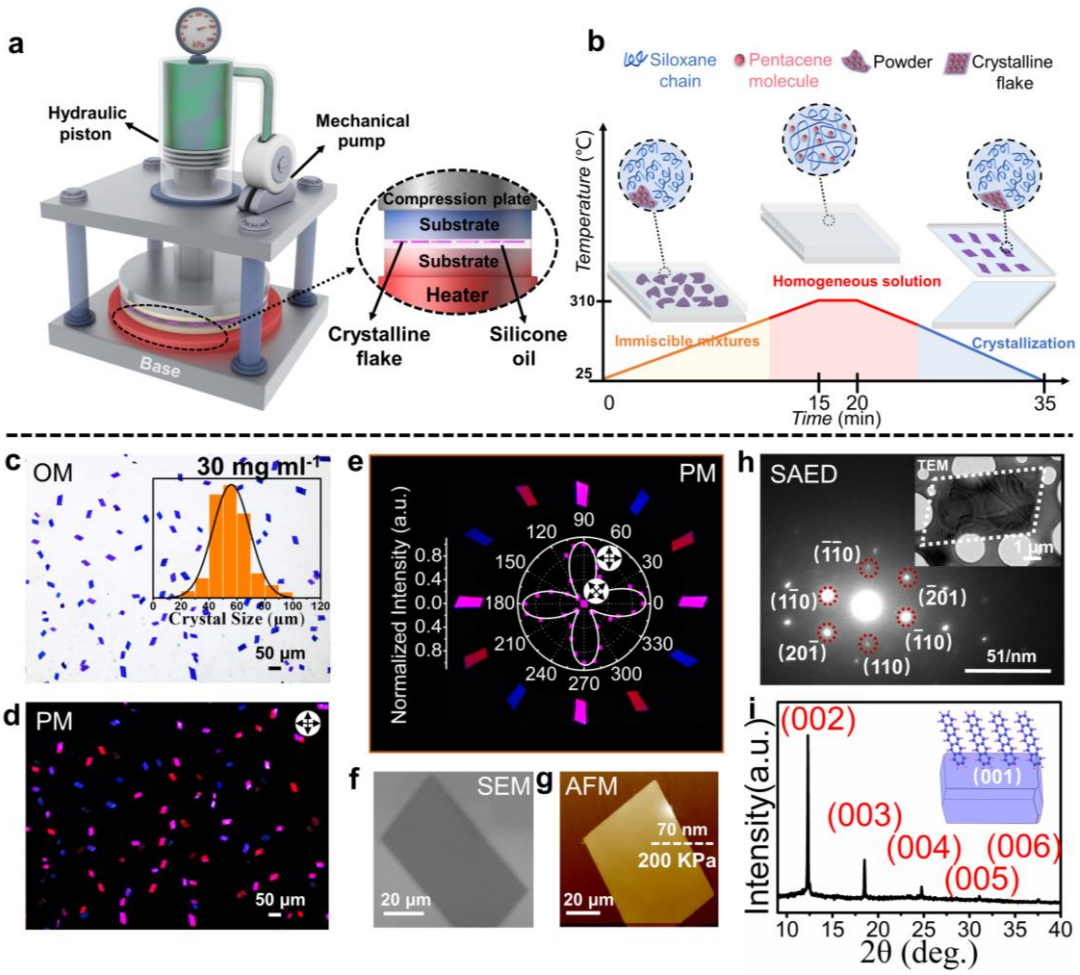

Figure 1. Illustration of CFG exemplified by growing pentacene single crystalline flakes with silicone oil as polymer flux. a. Schematic of the growth apparatus. The enlarged image depicts the growth system between a bottom heater and an upper compression plate connected to a hydraulic piston. **b.** Temperature program and mixing status of polydimethylsiloxane (blue curves) and pentacene (pink dot for individual molecule, purple irregular shape for powder, and purple rhomboid for single crystal) in the corresponding immiscible (light yellow), homogeneous (light pink), and crystallization (light blue) stages during the growth process. (**c**) Optical and (**d**) cross-polarized optical microscopy images of the pentacene single crystalline flakes. The inset in **c** shows the size distribution of the grown pentacene crystalline flakes. **e.** Polarization angle-dependent reflection intensity of a pentacene single crystalline flake with a four-leaf clover pattern. (**f**) SEM and (**g**) AFM images of a pentacene single crystalline flake. **h.** TEM image of a small piece of pentacene flake and the corresponding SAED pattern. **i.** XRD pattern of the as-grown pentacene flakes, where the inset shows the equilibrium crystal morphology of pentacene.

This article is protected by copyright. All rights reserved.

15214095, ja, Downloaded from https://onlinelibrary.wiley.com/doi/10.1002/adma.202210685 by CochraneChina, Wiley Online Library on [06/01/2023]. See the Terms and Conditions (https://onlinelibrary.wiley.com/terms-and-conditions) on Wiley Online Library for rules of use; OA articles are governed by the applicable Creative Commons License

Accepted Article

15214095, ja, Downloaded from https://onlinelibrary.wiley.com/doi/10.1002/adma.202210685 by CochraneChina, Wiley Online Library on [06/01/2023]. See the Terms and Conditions (https://onlinelibrary.wiley.com/terms-and-conditions) on Wiley Online Library for rules of use; OA articles are governed by the applicable Creative Commons License

2.2. Dimensional Tunability of CFG and Processability of Grown Crystals

The lateral size of the crystalline flakes was determined by the supersaturation, where a slower cooling rate and higher concentration were found to produce a larger size (**Figure 2a**). Furthermore, the thickness of the crystalline flakes could effectively be regulated by the pressure applied to the substrate (with the thickness decreasing from 330 nm to 26 nm with an increase in pressure to a value close to 500 kPa, **Figure 2b**). In contrast, the number-density of the grown flakes was mainly controlled by the concentration, as shown in **Figures 2c** and **S5**. Under a concentration of 75 mg mL^{-1} and cooling rate of 10 °Cmin^{-1}, more than 2 × 10^5 flakes per square centimeter could be grown, showing the high-productivity of CFG.

The single-crystalline flakes grown with CFG could be integrated into various application scenarios through strategies like transfer and printing. **Figures 2d and 2e** present a demo where a dispersion ink containing crystalline flakes is used to print a film on a 5-inch Si/SiO_2 wafer and construct a large-scale field effect transistor array (the details are discussed in the Section 2.14 of Supporting Information. The results demonstrated that the deposition of the pre-formed single crystals dispensed with any crystallization protocols, but provided superior crystallinity and uniformity compared to the conventional printing of molecularly dispersed solution inks. Furthermore, CFG is potentially applicable to produce large lateral sized ultrathin crystalline films under extremely high pressure. Based on the principles of CFG and our preliminary experimental results (**Figure S28**), we propose a roadmap for large lateral sized single crystal by controlled growth from a single nucleus, or epitaxial growth from the patterned uniformly aligned van der Waals seeds (**Figure S29**). The details about the roadmap of large lateral sized single crystal growth are discussed in the Section 2.14.4 of Supporting Information.

This article is protected by copyright. All rights reserved.

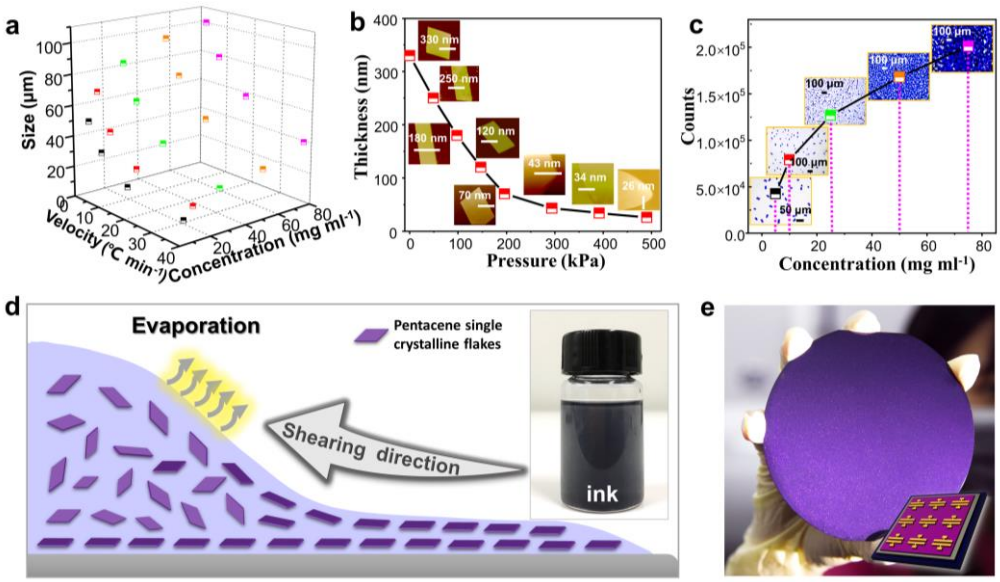

Figure 2. Effects of growth parameters on the dimensions and productivity of the single-crystalline flakes and integration of single-crystalline flakes into electronic devices. a. Lateral size dependence on the concentration and cooling rate. **b.** Dependence of single-crystalline flake thickness on the applied pressure. **c.** Dependence of the productivity (number-density per square centimeter) on the concentration. **d.** A photo of a suspension ink of pentacene flakes and schematic of printing the single-crystalline flakes onto a substrate through a liquid surface shear method. **e.** Photograph of printed pentacene crystalline flake film on a 5-inch Si/SiO_2 wafer substrate. Inset is a schematic of the FET device configuration with pentacene crystalline flakes as the *p*-channel semiconductor and Au as the source and drain electrodes.

2.3. Synergistic Effects of Polymer Flux and Pressure, and Phase Miscibility

In situ observation of the CFG was recorded to intuitively capture the growth process under a hot stage microscope. (see **Figure 3a** and **Supplementary Video 3** for pentacene, and **Figure S7** and **Supplementary Videos 1** and **2** for the other materials). When heated to ~243 °C, the pentacene solids started to dissolve from the periphery; after a temperature ramp of ~60 °C, the pentacene was completely dissolved in the silicone oil, and a homogenous system was obtained. It is worth noting that the single-crystalline pentacene flakes crystallized from the miscible solution by expanding their regular edges outward after a hysteresis of ~40 °C in the cooling stage. The dissolution and crystallization could be repeated for multiple cycles (**Supplementary Video 3**), indicating a confined

This article is protected by copyright. All rights reserved.

Accepted Article

15214095, ja, Downloaded from https://onlinelibrary.wiley.com/doi/10.1002/adma.202210685 by CochraneChina, Wiley Online Library on [06/01/2023]. See the Terms and Conditions (https://onlinelibrary.wiley.com/terms-and-conditions) on Wiley Online Library for rules of use; OA articles are governed by the applicable Creative Commons License

diffusion range for the CFG and good protection against the degradation of the susceptible pentacene.

The two key factors for the CFG, the polymer flux and pressure, were essential to guarantee the stability of the materials during growth. The thermo gravimetry/differential scan calorimeter (TG–DSC) results shown in **Figure 3b** indicate their thermal properties under different conditions, demonstrating their protective effect. When both the silicone flux and pressure were introduced, the decomposition point of pentacene shifted to a temperature that was nearly 100 °C higher than that in the case without these two factors (458.4 °C vs. 364.8 °C), and no endo- or exothermic peak was recorded, suggesting that the isothermal melting of the pentacene may have been replaced by its gradual dissolution into the polymer flux. These results indicated that the compressed polymer flux provided the incorporated materials with excellent protection against oxidation and decomposition.

In a realistic growth process, if the polymer flux was absent and the raw materials were simply sandwiched between two compressed substrates, no single crystals could be produced, but only polycrystals, spherulites, or even amorphous solids (**Figure S8**). The schematics in **Figure 3c** outline the synergistic effects of the polymer flux and pressure. Coupling these two factors created a confined growth medium, which facilitated the assembly of the dissolved molecules into 2D single crystals and protected the materials from degradation during the growth process (**Figure S9**).

This article is protected by copyright. All rights reserved.

Accepted Article

15214095, ja, Downloaded from https://onlinelibrary.wiley.com/doi/10.1002/adma.202210685 by CochraneChina, Wiley Online Library on [06/01/2023]. See the Terms and Conditions (https://onlinelibrary.wiley.com/terms-and-conditions) on Wiley Online Library for rules of use; OA articles are governed by the applicable Creative Commons License

Accepted Article

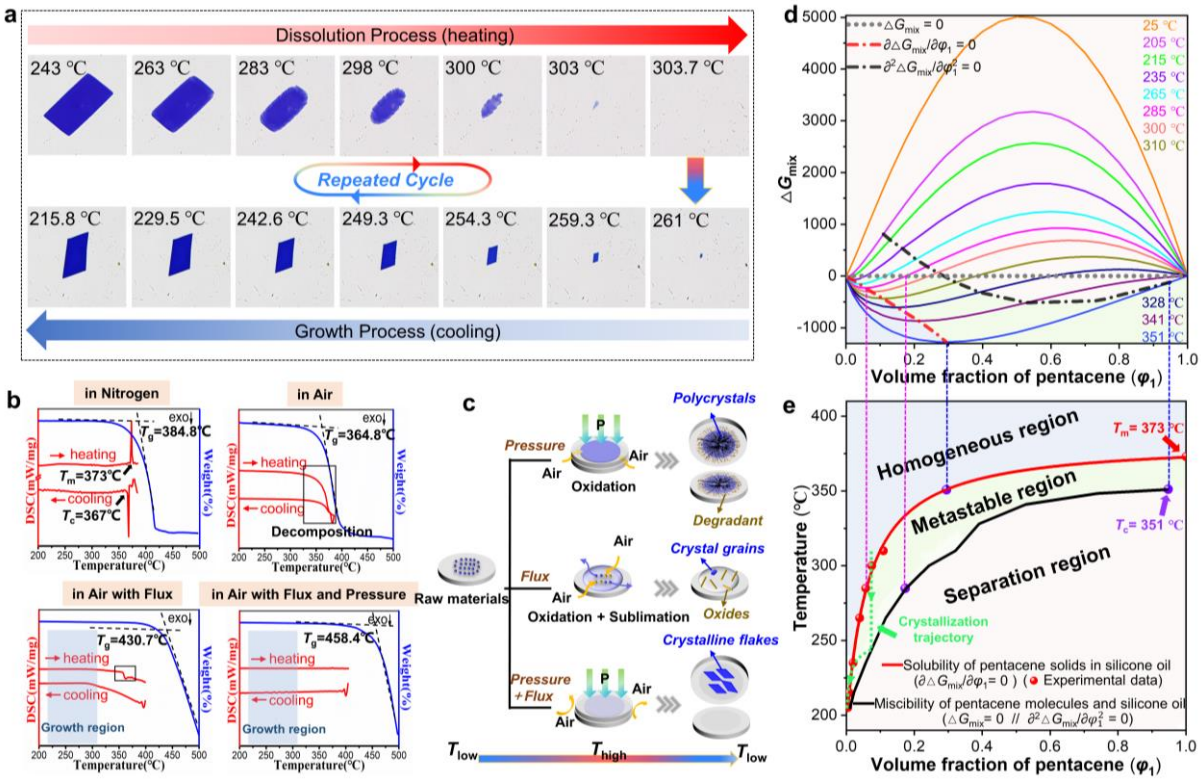

Figure 3. Compressed flux growth process identifying the synergistic effects of the polymer flux and pressure, and the phase miscibility. a. In situ record of the dissolution and crystallization of a pentacene single crystalline flake in silicone oil sandwiched between two glass substrates. It should be noted that the re-crystallized flake became smaller and thicker than the original flake because of the slight pressure to compromise with the in situ observation. **b.** TG–DSC measurements of pentacene under different conditions. **c.** Synergistic effects of polymer flux and pressure in preventing material degradation and facilitating 2D assembly. (**d** and **e**) Phase diagrams of mixing free energy (ΔG_{mix}) (**d**) and temperature (**e**) as a function of the pentacene fraction (φ_1) in silicone oil.

To illustrate the miscibility of the polymer flux with small molecular solids, the phase diagrams of a silicone oil–pentacene system were charted based on the Flory–Huggins theory[25, 26] and measured solubility curve of our growth experiment. The curves for the relative Gibbs free energy of mixing (ΔG_{mix}) as a function of the fraction of pentacene (φ_1) at different temperatures are shown in **Figure 3d**. Based on the miscibility criteria ($\Delta G_{mix} < 0$ and $\partial^2 \Delta G_{mix}/\partial \varphi_1^2 > 0$) and solubility criterion ($\partial \Delta G_{mix}/\partial \varphi_1 = 0$), the phase diagram of the binary system could be partitioned into separation, metastable, and homogeneous regions. These three regions corresponding to the temperature–

This article is protected by copyright. All rights reserved.

15214095, ja, Downloaded from https://onlinelibrary.wiley.com/doi/10.1002/adma.202210685 by CochraneChina, Wiley Online Library on [06/01/2023]. See the Terms and Conditions (https://onlinelibrary.wiley.com/terms-and-conditions) on Wiley Online Library for rules of use; OA articles are governed by the applicable Creative Commons License

Accepted Article

fraction of pentacene phase diagram (**Figure 3e**) are analogous to the case of crystallization from a solution or melt.[27, 28] The experimental solubilities (red dots) fit well with the calculated solubility curve, where a solubility of 5 mg/mL requires a temperature of ~205 °C, and it reached 150 mg mL^{-1} at ~310 °C. Above critical temperature T_c (calculated to be ~351 °C), pentacene and silicone oil become fully miscible. This miscibility was maintained in the metastable region, corresponding to the supercooling and temperature hysteresis in the growth stage. The green dotted trajectory in **Figure 3e** illustrates a CFG practice starting from 310 °C at a concentration of 100 mg mL^{-1}. Once the temperature decreased to the boundary between the metastable and separation regions, nucleation occurred, and the continuous growth decreased the supersaturation until a total phase separation at a temperature of ~200 °C. The details of the temperature dependent mixing free energy (ΔG_{mix}) of the silicone oil–pentacene system are discussed in the Section 2.7 of Supporting Information. It should be noted that during the CFG, the practicable growth temperature lies closely below the melting point (T_m) of the respective material, as shown in **Figure S23** and **Table S4**, which is reminiscent of traditional flux growth utilizing a melt of metals or inorganics as a high-temperature solvent for the crystallization of oxides and intermetallic compounds. Moreover, the polymer in CFG behaves distinctly from the inorganic "flux" or small molecular "solvent," because of its specific miscibility with the solutes, *i.e.*, it is totally insoluble at a low temperature while highly miscible near T_m. Thus, the adoption of a stable and inert polymer flux results in a significant solubility change upon temperature variation, endowing CFG with the prominent advantage of a nearly 100% recovery yield.

2.4. Selection of Polymer Flux and Generality of CFG

In addition to silicone oil, it has been proven that polymers possessing unique properties such as high thermal and mechanical stability, chemical inertness, and a negligible vapor pressure would qualify as fluxes. Other common polymers such as polyethylene glycol (PEG), poly(propyleneglycol)bis(2-aminopropylether) (PEA), polystyrene (PS), poly(methyl metacrylate) (PMMA), and polyvinylidene fluoride (PVDF) could be used as fluxes in CFG to accommodate different kinds of crystals (**Figure 4a**). By virtue of the multiple choices for polymer fluxes, CFG

This article is protected by copyright. All rights reserved.

15214095, ja, Downloaded from https://onlinelibrary.wiley.com/doi/10.1002/adma.202210685 by CochraneChina, Wiley Online Library on [06/01/2023]. See the Terms and Conditions (https://onlinelibrary.wiley.com/terms-and-conditions) on Wiley Online Library for rules of use; OA articles are governed by the applicable Creative Commons License

Accepted Article

applies to a broad range of materials. The details are provided in **Table S3** and discussed in the Section 2.9 of Supporting Information. We tested twenty kinds of materials, including organic semiconductors, pharmaceuticals, metal–organic complexes, and inorganics (**Figure 4b**). The same compound could be grown using a series of polymer fluxes. Likewise, one polymer flux was compatible with a series of compounds. The applicable polymer fluxes are presented above each material. It was found that CFG had a powerful growth ability: the hardly-dissolvable molecules such as pentacene (12) and dinaphtho[2,3-b:2′,3′-f]thieno[3,2-b]thiophene (DNTT, 14) could be effectively grown into crystalline flakes; and poorly crystallizable molecules like 2,2′,7,7′-tetrakis(N,N-di-p-methoxy-phenylamine)-9,9′-spirobifluorene (spiro-OMeTAD, 11) were completely crystallized into elongated hexagonal crystals within 10 min. Moreover, CFG restricts the growing system to a vertically confined space, which favors low-dimensional growth regardless of the intrinsic crystal habits. **Figure 4c** shows PM images of the as-grown crystals, wherein the twenty kinds of crystals exhibit low-dimensional morphologies. For example, when using tetraphenylethene (TPE, 7), which possesses an intrinsic three-dimensional habit in solution and vapor growth,[29, 30] CFG produced crystalline ribbons with aspect ratios of up to several thousand (**Figure S19**). The preferred out-of-plane orientation (see labeled equilibrium crystal morphology) of the crystals was further manifested by the XRD spectra (**Figure S18**).

In addition to its high efficiency and wide universality, another merit of CFG is the narrow size distribution of the grown crystals (**Figures 4d** and **S20–21**). We attribute the control of the lateral size to two factors: quasi-homogeneous nucleation and diffusion-limited growth. The effective lateral diffusion coefficient of pentacene in silicone oil in CFG was estimated to be ~0.09 $\mu m^2 s^{-1}$ according to the Stokes−Einstein relation[31, 32], which was coincident with the typical growth rate (0.2–0.3 $\mu m\ s^{-1}$) measured in the experiments (**Figures 3a** and **S4**). The details of the nucleation and diffusion during CFG are discussed in the Section 2.1 of Supporting Information.

This article is protected by copyright. All rights reserved.

15214095, ja, Downloaded from https://onlinelibrary.wiley.com/doi/10.1002/adma.202210685 by CochraneChina, Wiley Online Library on [06/01/2023]. See the Terms and Conditions (https://onlinelibrary.wiley.com/terms-and-conditions) on Wiley Online Library for rules of use; OA articles are governed by the applicable Creative Commons License

Accepted Article

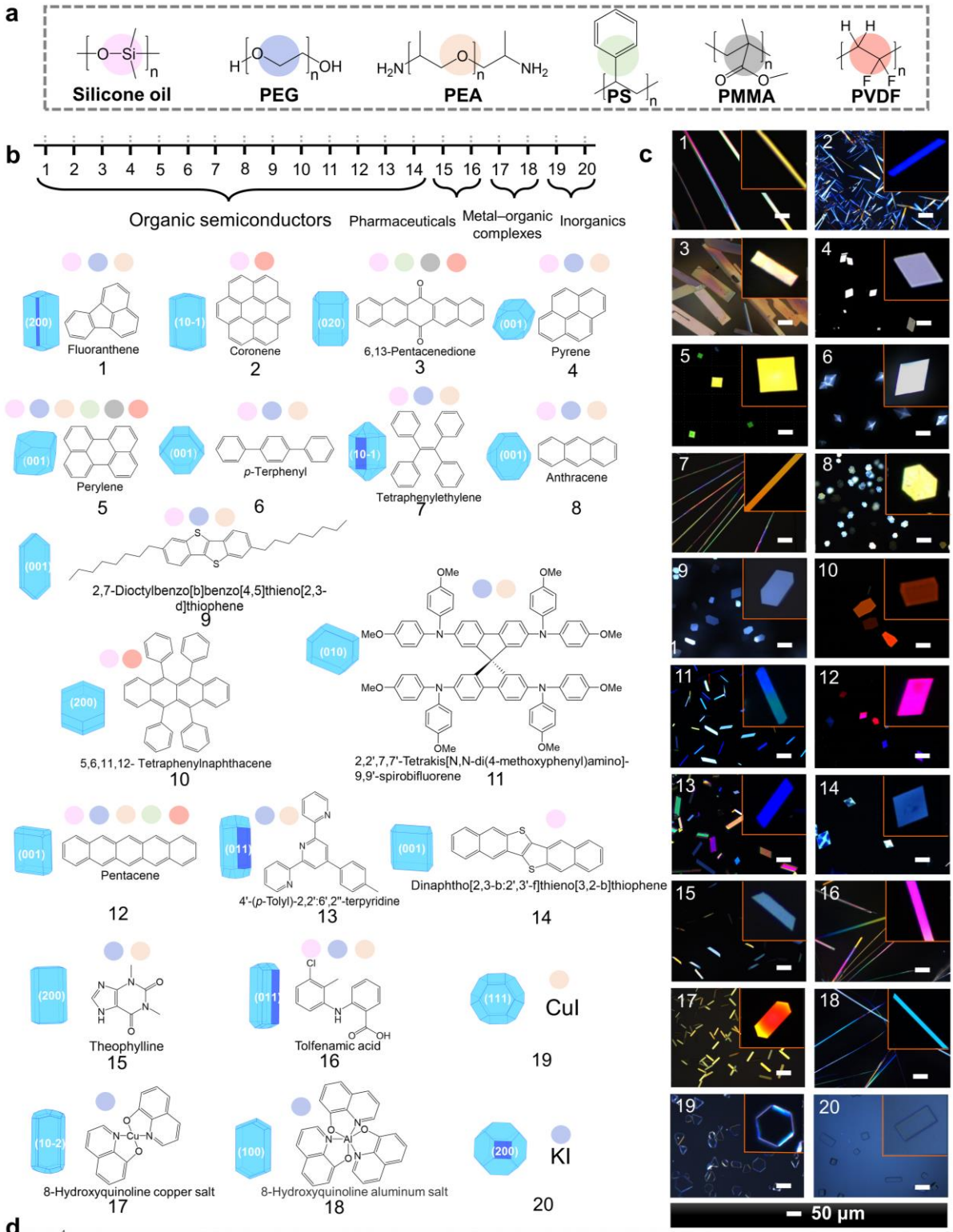

15214095, ja, Downloaded from https://onlinelibrary.wiley.com/doi/10.1002/adma.202210685 by CochraneChina, Wiley Online Library on [06/01/2023]. See the Terms and Conditions (https://onlinelibrary.wiley.com/terms-and-conditions) on Wiley Online Library for rules of use; OA articles are governed by the applicable Creative Commons License

Accepted Article

Figure 4. Universal application of CFG to various materials with the adoption of different polymer fluxes. a. Polymers used as fluxes. The different colored circles on each chemical structure indicate the compatibility of different polymers with the corresponding material in (**b**). **b.** Chemical structures of the 20 kinds of compounds used for crystal growth in CFG, including organic semiconductors (1–14), pharmaceuticals (15, 16), metal–organic complexes (17, 18), and inorganics (19, 20). The equilibrium crystal morphology labeled with the main crystal plane is displayed beside each chemical. **c.** Polarized optical microscope images of the respective crystals grown by CFG, where the inset in each panel shows an enlarged representation of an individual single crystal (scale bar: 50 μm). **d.** Size distributions of the grown crystals. The elements of the box plots include the 25% and 75% quartiles (edges of the box), median (midline), and maximum/minimum values (whiskers).

3. Conclusion

In conclusion, we demonstrated a high-yield growth method for a wide range of functional crystals, overcoming the low efficiency, poor controllability, and solubility-limitation of traditional vapor and solution methods (comparisons are summarized in **Table S7**). Because the lack of efficient preparation methods for single crystals with defined dimensions has hampered both their research prospects and practical applications for several decades, the significance of CFG lies in its general applicability to the mass production of single crystals with dimensional uniformity. Based on the large-scale production of micro-single crystals, the integration of these uniform crystal “bricks” into various application scenarios holds promise.

4. Experimental Section

The details of the experiments and methods are provided in the Supporting Information.

Supporting Information

Supporting Information is available from the Wiley Online Library or from the author.

This article is protected by copyright. All rights reserved.

15214095, ja, Downloaded from https://onlinelibrary.wiley.com/doi/10.1002/adma.202210685 by CochraneChina, Wiley Online Library on [06/01/2023]. See the Terms and Conditions (https://onlinelibrary.wiley.com/terms-and-conditions) on Wiley Online Library for rules of use; OA articles are governed by the applicable Creative Commons License

Accepted Article

Acknowledgements

We are grateful for the financial support of this work provided by the National Natural Science Foundation of China (Grants 52273185, 51973106 and 51932004), the National Key Research and Development Program of China (Grants 2018YFB0406502), the 111 Project 2.0 in China (Grant PB2018013), Distinguished Young Scholars of Shandong Province (ZR2019JQ03), and Shandong University multidisciplinary research and innovation team of young scholars. C.G. thanks Prof. Shi-bing Liu and Hai-ying Song from the Beijing University of Technology for their help in the theoretical analysis.

Received: ((will be filled in by the editorial staff))
Revised: ((will be filled in by the editorial staff))
Published online: ((will be filled in by the editorial staff))

References

[1] S. Datta, D. J. Grant, *Nat. Rev. Drug Discov*. **2004**, *3*, 42.

[2] R. D. Blake, J. R. Fresco, R. Langridge, *Nature* **1970**, *225*, 32.

[3] R. Dong, X. Feng, *Nat. Mater.* **2021**, *20*, 122.

[4] G. Chen, Y. Peng, G. Zheng, Z. Qi, M. Wang, H. Yu, C. Dong, C. Liu, *Nat. mater.* **2016**, *15*, 876.

[5] N. K. Arakere, G. Swanson, *J. Eng. Gas Turbines Power* **2002**, *124*, 161.

[6] S. Nishino, J. A. Powell, H. A. Will, *ApPhL* **1983**, *42*, 460.

[7] F. Yang, S. Cheng, X. Zhang, X. Ren, R. Li, H. Dong, W. Hu, *Adv. Mater.* **2018**, *30*, 1702415.

[8] A. Yamamura, S. Watanabe, M. Uno, M. Mitani, C. Mitsui, J. Tsurumi, N. Isahaya, Y. Kanaoka, T. Okamoto, J. Takeya, *Sci. Adv.* **2018**, *4*, 5758.

This article is protected by copyright. All rights reserved.

15214095, ja, Downloaded from https://onlinelibrary.wiley.com/doi/10.1002/adma.202210685 by CochraneChina, Wiley Online Library on [06/01/2023]. See the Terms and Conditions (https://onlinelibrary.wiley.com/terms-and-conditions) on Wiley Online Library for rules of use; OA articles are governed by the applicable Creative Commons License

[9] J. Tao, D. Liu, J. Jing, H. Dong, L. Liu, B. Xu, W. Tian, *Adv. Mater.* **2021**, *33*, 2105466.

[10] A. L. Briseno, S. C. Mannsfeld, M. M. Ling, S. Liu, R. J. Tseng, C. Reese, M. E. Roberts, Y. Yang, F. Wudl, Z. Bao, *Nature* **2006**, *444*, 913.

[11] I. Kao, C. Chung, *Wafer Manufacturing: Shaping of Single Crystal Silicon Wafers*, John Wiley & Sons, **2021**.

[12] M. G. Kanatzidis, R. Pöttgen, W. Jeitschko, *Angew. Chem. Int. Ed.* **2005**, *44*, 6996.

[13] D. E. Bugaris, H. C. zur Loye, *Angew. Chem. Int. Ed.* **2012**, *51*, 3780.

[14] Z. Lin, Y. Liu, U. Halim, M. Ding, Y. Liu, Y. Wang, C. Jia, P. Chen, X. Duan, C. Wang, *Nature* **2018**, *562*, 254.

[15] Y. Diao, B. C. Tee, G. Giri, J. Xu, D. H. Kim, H. A. Becerril, R. M. Stoltenberg, T. H. Lee, G. Xue, S. C. Mannsfeld, *Nat. mater.* **2013**, *12*, 665.

[16] H. Minemawari, T. Yamada, H. Matsui, J. y. Tsutsumi, S. Haas, R. Chiba, R. Kumai, T. Hasegawa, *Nature* **2011**, *475*, 364.

[17] X. Ye, Y. Liu, Q. Guo, Q. Han, C. Ge, S. Cui, L. Zhang, X. Tao, *Nat. Commun.* **2019**, *10*, 1.

[18] H. Gao, Y. Qiu, J. Feng, S. Li, H. Wang, Y. Zhao, X. Wei, X. Jiang, Y. Su, Y. Wu, *Nat. Commun.* **2019**, *10*, 1.

[19] P. Zhang, X. Wang, H. Jiang, Y. Zhang, Q. He, K. Si, B. Li, F. Zhao, A. Cui, Y. Wei, *Nat. Synth* **2022**, 1, 864.

[20] H. Kim, Y. Yoo, *Nat. Synth* **2022**, 1, 833.

[21] W. Noll, *Chemistry and technology of silicones*, Elsevier, **2012**.

[22] J. J. Chruściel, *Silicon-based Polymers and Materials*, Walter de Gruyter GmbH & Co KG, **2022**.

[23] C. Kim, A. Facchetti, T. J. Marks, *Sci* **2007**, *318*, 76.

This article is protected by copyright. All rights reserved.

Accepted Article

15214095, ja, Downloaded from https://onlinelibrary.wiley.com/doi/10.1002/adma.202210685 by CochraneChina, Wiley Online Library on [06/01/2023]. See the Terms and Conditions (https://onlinelibrary.wiley.com/terms-and-conditions) on Wiley Online Library for rules of use; OA articles are governed by the applicable Creative Commons License

[24] F.-J. Meyer zu Heringdorf, M. Reuter, R. Tromp, *Nature* **2001**, *412*, 517.

[25] P. J. Flory, *Principles of polymer chemistry*, Cornell university press, **1953**.

[26] M. L. Huggins, *Ann. N. Y. Acad. Sci.* **1942**, *43*, 1.

[27] K. M. Ng, R. Gani, K. Dam-Johansen, *Chemical product design: towards a perspective through case studies*, Elsevier, **2006**.

[28] A. Avdeef, E. Fuguet, A. Llinàs, C. Ràfols, E. Bosch, G. Völgyi, T. Verbić, E. Boldyreva, K. Takács-Novák, *ADMET and DMPK* **2016**, *4*, 117.

[29] H. Yuan, K. Wang, K. Yang, B. Liu, B. Zou, *J. Phys. Chem. Lett.* **2014**, *5*, 2968.

[30] X. Ye, Y. Liu, Q. Han, C. Ge, S. Cui, L. Zhang, X. Zheng, G. Liu, J. Liu, D. Liu, *Chem. Mater.* **2018**, *30*, 412.

[31] G. G. Stokes, **1851**.

[32] A. Einstein, *AnP* **1905**, *17*, 208.

This article is protected by copyright. All rights reserved.

Accepted Article

15214095, ja, Downloaded from https://onlinelibrary.wiley.com/doi/10.1002/adma.202210685 by CochraneChina, Wiley Online Library on [06/01/2023]. See the Terms and Conditions (https://onlinelibrary.wiley.com/terms-and-conditions) on Wiley Online Library for rules of use; OA articles are governed by the applicable Creative Commons License

Accepted Article

WILEY-VCH

Polymer-Assisted Compressed Flux Growth: A Universal and High-Yield Method for Dimension-Controlled Single Crystals

Chao Ge[1,2,†], Xiaoxin Zheng[1,†], Qing Guo[1], Yang Liu[1,*], and Xutang Tao[1,*]

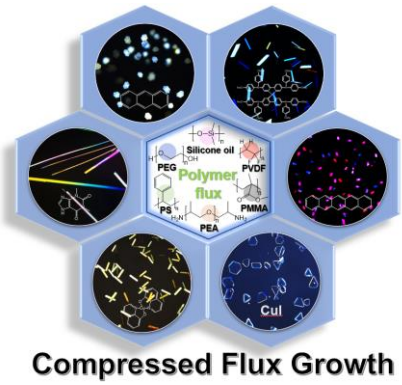

Table of contents

A high-yield crystal growth method that utilized a polymer flux in a compressed growth space was invented to cast molecules or precursors into dimension-defined single crystals. This compressed flux growth (CFG) is universally applicable to various materials and scalable to mass production, and the grown single crystals could be directly integrated into electronic devices.

This article is protected by copyright. All rights reserved.

15214095, ja, Downloaded from https://onlinelibrary.wiley.com/doi/10.1002/adma.202210685 by CochraneChina, Wiley Online Library on [06/01/2023]. See the Terms and Conditions (https://onlinelibrary.wiley.com/terms-and-conditions) on Wiley Online Library for rules of use; OA articles are governed by the applicable Creative Commons License